

Search for the weak decay $\eta' \rightarrow K^\pm \pi^\mp$ and precise measurement of the branching fraction $\mathcal{B}(J/\psi \rightarrow \phi \eta')$

M. Ablikim¹, M. N. Achasov^{9,f}, X. C. Ai¹, O. Albayrak⁵, M. Albrecht⁴, D. J. Ambrose⁴⁴, A. Amoroso^{49A,49C}, F. F. An¹, Q. An^{46,a}, J. Z. Bai¹, R. Baldini Ferroli^{20A}, Y. Ban³¹, D. W. Bennett¹⁹, J. V. Bennett⁵, M. Bertani^{20A}, D. Bettini^{21A}, J. M. Bian⁴³, F. Bianchi^{49A,49C}, E. Boger^{23,d}, I. Boyko²³, R. A. Briere⁵, H. Cai⁵¹, X. Cai^{1,a}, O. Cakir^{40A,b}, A. Calcaterra^{20A}, G. F. Cao¹, S. A. Cetin^{40B}, J. F. Chang^{1,a}, G. Chelkov^{23,d,e}, G. Chen¹, H. S. Chen¹, H. Y. Chen², J. C. Chen¹, M. L. Chen^{1,a}, S. J. Chen²⁹, X. Chen^{1,a}, X. R. Chen²⁶, Y. B. Chen^{1,a}, H. P. Cheng¹⁷, X. K. Chu³¹, G. Cibinetto^{21A}, H. L. Dai^{1,a}, J. P. Dai³⁴, A. Dbeyssi¹⁴, D. Dedovich²³, Z. Y. Deng¹, A. Denig²², I. Denysenko²³, M. Destefanis^{49A,49C}, F. De Mori^{49A,49C}, Y. Ding²⁷, C. Dong³⁰, J. Dong^{1,a}, L. Y. Dong¹, M. Y. Dong^{1,a}, S. X. Du⁵³, P. F. Duan¹, J. Z. Fan³⁹, J. Fang^{1,a}, S. S. Fang¹, X. Fang^{46,a}, Y. Fang¹, L. Fava^{49B,49C}, F. Feldbauer²², G. Felici^{20A}, C. Q. Feng^{46,a}, E. Fioravanti^{21A}, M. Fritsch^{14,22}, C. D. Fu¹, Q. Gao¹, X. Y. Gao², Y. Gao³⁹, Z. Gao^{46,a}, I. Garzia^{21A}, K. Goetzen¹⁰, W. X. Gong^{1,a}, W. Gradl²², M. Greco^{49A,49C}, M. H. Gu^{1,a}, Y. T. Gu¹², Y. H. Guan¹, A. Q. Guo¹, L. B. Guo²⁸, Y. Guo¹, Y. P. Guo²², Z. Haddadi²⁵, A. Hafner²², S. Han⁵¹, X. Q. Hao¹⁵, F. A. Harris⁴², K. L. He¹, X. Q. He⁴⁵, T. Held⁴, Y. K. Heng^{1,a}, Z. L. Hou¹, C. Hu²⁸, H. M. Hu¹, J. F. Hu^{49A,49C}, T. Hu^{1,a}, Y. Hu¹, G. M. Huang⁶, G. S. Huang^{46,a}, J. S. Huang¹⁵, X. T. Huang³³, Y. Huang²⁹, T. Hussain⁴⁸, Q. Ji¹, Q. P. Ji³⁰, X. B. Ji¹, X. L. Ji^{1,a}, L. W. Jiang⁵¹, X. S. Jiang^{1,a}, X. Y. Jiang³⁰, J. B. Jiao³³, Z. Jiao¹⁷, D. P. Jin^{1,a}, S. Jin¹, T. Johansson⁵⁰, A. Julin⁴³, N. Kalantar-Nayestanaki²⁵, X. L. Kang¹, X. S. Kang³⁰, M. Kavatsyuk²⁵, B. C. Ke⁵, P. Kiese²², R. Kliemt¹⁴, B. Kloss²², O. B. Kolcu^{40B,i}, B. Kopf⁴, M. Kornicer⁴², W. Kühn²⁴, A. Kupsc⁵⁰, J. S. Lange²⁴, M. Lara¹⁹, P. Larin¹⁴, C. Leng^{49C}, C. Li⁵⁰, Cheng Li^{46,a}, D. M. Li⁵³, F. Li^{1,a}, F. Y. Li³¹, G. Li¹, H. B. Li¹, J. C. Li¹, Jin Li³², K. Li³³, K. Li¹³, Lei Li³, P. R. Li⁴¹, T. Li³³, W. D. Li¹, W. G. Li¹, X. L. Li³³, X. M. Li¹², X. N. Li^{1,a}, X. Q. Li³⁰, Z. B. Li³⁸, H. Liang^{46,a}, Y. F. Liang³⁶, Y. T. Liang²⁴, G. R. Liao¹¹, D. X. Lin¹⁴, B. J. Liu¹, C. X. Liu¹, F. H. Liu³⁵, Fang Liu¹, Feng Liu⁶, H. B. Liu¹², H. H. Liu¹, H. H. Liu¹⁶, H. M. Liu¹, J. Liu¹, J. B. Liu^{46,a}, J. P. Liu⁵¹, J. Y. Liu¹, K. Liu³⁹, K. Y. Liu²⁷, L. D. Liu³¹, P. L. Liu^{1,a}, Q. Liu⁴¹, S. B. Liu^{46,a}, X. Liu²⁶, Y. B. Liu³⁰, Z. A. Liu^{1,a}, Zhiqing Liu²², H. Loehner²⁵, X. C. Lou^{1,a,h}, H. J. Lu¹⁷, J. G. Lu^{1,a}, Y. Lu¹, Y. P. Lu^{1,a}, C. L. Luo²⁸, M. X. Luo⁵², T. Luo⁴², X. L. Luo^{1,a}, X. R. Lyu⁴¹, F. C. Ma²⁷, H. L. Ma¹, L. L. Ma³³, Q. M. Ma¹, T. Ma¹, X. N. Ma³⁰, X. Y. Ma^{1,a}, F. E. Maas¹⁴, M. Maggiora^{49A,49C}, Y. J. Mao³¹, Z. P. Mao¹, S. Marcello^{49A,49C}, J. G. Messchendorp²⁵, J. Min^{1,a}, R. E. Mitchell¹⁹, X. H. Mo^{1,a}, Y. J. Mo⁶, C. Morales Morales¹⁴, K. Moriya¹⁹, N. Yu. Muchnoi^{9,f}, H. Muramatsu⁴³, Y. Nefedov²³, F. Nerling¹⁴, I. B. Nikolaev^{9,f}, Z. Ning^{1,a}, S. Nisar⁸, S. L. Niu^{1,a}, X. Y. Niu¹, S. L. Olsen³², Q. Ouyang^{1,a}, S. Pacetti^{20B}, P. Patteri^{20A}, M. Pelizaeus⁴, H. P. Peng^{46,a}, K. Peters¹⁰, J. Pettersson⁵⁰, J. L. Ping²⁸, R. G. Ping¹, R. Poling⁴³, V. Prasad¹, M. Qi²⁹, S. Qian^{1,a}, C. F. Qiao⁴¹, L. Q. Qin³³, N. Qin⁵¹, X. S. Qin¹, Z. H. Qin^{1,a}, J. F. Qiu¹, K. H. Rashid⁴⁸, C. F. Redmer²², M. Ripka²², G. Rong¹, Ch. Rosner¹⁴, X. D. Ruan¹², V. Santoro^{21A}, A. Sarantsev^{23,g}, M. Savrié^{21B}, K. Schoenning⁵⁰, S. Schumann²², W. Shan³¹, M. Shao^{46,a}, C. P. Shen², P. X. Shen³⁰, X. Y. Shen¹, H. Y. Sheng¹, W. M. Song¹, X. Y. Song¹, S. Sosio^{49A,49C}, S. Spataro^{49A,49C}, G. X. Sun¹, J. F. Sun¹⁵, S. S. Sun¹, Y. J. Sun^{46,a}, Y. Z. Sun¹, Z. J. Sun^{1,a}, Z. T. Sun¹⁹, C. J. Tang³⁶, X. Tang¹, I. Tapan^{40C}, E. H. Thorndike⁴⁴, M. Tiemens²⁵, M. Ullrich²⁴, I. Uman^{40B}, G. S. Varner⁴², B. Wang³⁰, D. Wang³¹, D. Y. Wang³¹, K. Wang^{1,a}, L. L. Wang¹, L. S. Wang¹, M. Wang³³, P. Wang¹, P. L. Wang¹, S. G. Wang³¹, W. Wang^{1,a}, X. F. Wang³⁹, Y. D. Wang¹⁴, Y. F. Wang^{1,a}, Y. Q. Wang²², Z. Wang^{1,a}, Z. G. Wang^{1,a}, Z. H. Wang^{46,a}, Z. Y. Wang¹, T. Weber²², D. H. Wei¹¹, J. B. Wei³¹, P. Weidenkaff²², S. P. Wen¹, U. Wiedner⁴, M. Wolke⁵⁰, L. H. Wu¹, Z. Wu^{1,a}, L. G. Xia³⁹, Y. Xia¹⁸, D. Xiao¹, H. Xiao⁴⁷, Z. J. Xiao²⁸, Y. G. Xie^{1,a}, Q. L. Xiu^{1,a}, G. F. Xu¹, L. Xu¹, Q. J. Xu¹³, X. P. Xu³⁷, L. Yan^{46,a}, W. B. Yan^{46,a}, W. C. Yan^{46,a}, Y. H. Yan¹⁸, H. J. Yang³⁴, H. X. Yang¹, L. Yang⁵¹, Y. Yang⁶, Y. X. Yang¹¹, M. Ye^{1,a}, M. H. Ye⁷, J. H. Yin¹, B. X. Yu^{1,a}, C. X. Yu³⁰, J. S. Yu²⁶, C. Z. Yuan¹, W. L. Yuan²⁹, Y. Yuan¹, A. Yuncu^{40B,c}, A. A. Zafar⁴⁸, A. Zallo^{20A}, Y. Zeng¹⁸, B. X. Zhang¹, B. Y. Zhang^{1,a}, C. Zhang²⁹, C. C. Zhang¹, D. H. Zhang¹, H. H. Zhang³⁸, H. Y. Zhang^{1,a}, J. J. Zhang¹, J. L. Zhang¹, J. Q. Zhang¹, J. W. Zhang^{1,a}, J. Y. Zhang¹, J. Z. Zhang¹, K. Zhang¹, L. Zhang¹, X. Y. Zhang³³, Y. Zhang¹, Y. N. Zhang⁴¹, Y. H. Zhang^{1,a}, Y. T. Zhang^{46,a}, Yu Zhang⁴¹, Z. H. Zhang⁶, Z. P. Zhang⁴⁶, Z. Y. Zhang⁵¹, G. Zhao¹, J. W. Zhao^{1,a}, J. Y. Zhao¹, J. Z. Zhao^{1,a}, Lei Zhao^{46,a}, Ling Zhao¹, M. G. Zhao³⁰, Q. Zhao¹, Q. W. Zhao¹, S. J. Zhao⁵³, T. C. Zhao¹, Y. B. Zhao^{1,a}, Z. G. Zhao^{46,a}, A. Zhemchugov^{23,d}, B. Zheng⁴⁷, J. P. Zheng^{1,a}, W. J. Zheng³³, Y. H. Zheng⁴¹, B. Zhong²⁸, L. Zhou^{1,a}, X. Zhou⁵¹, X. K. Zhou^{46,a}, X. R. Zhou^{46,a}, X. Y. Zhou¹, K. Zhu¹, K. J. Zhu^{1,a}, S. Zhu¹, S. H. Zhu⁴⁵, X. L. Zhu³⁹, Y. C. Zhu^{46,a}, Y. S. Zhu¹, Z. A. Zhu¹, J. Zhuang^{1,a}, L. Zotti^{49A,49C}, B. S. Zou¹, J. H. Zou¹

(BESIII Collaboration)

- ¹ *Institute of High Energy Physics, Beijing 100049, People's Republic of China*
- ² *Beihang University, Beijing 100191, People's Republic of China*
- ³ *Beijing Institute of Petrochemical Technology, Beijing 102617, People's Republic of China*
- ⁴ *Bochum Ruhr-University, D-44780 Bochum, Germany*
- ⁵ *Carnegie Mellon University, Pittsburgh, Pennsylvania 15213, USA*
- ⁶ *Central China Normal University, Wuhan 430079, People's Republic of China*
- ⁷ *China Center of Advanced Science and Technology, Beijing 100190, People's Republic of China*
- ⁸ *COMSATS Institute of Information Technology, Lahore, Defence Road, Off Raiwind Road, 54000 Lahore, Pakistan*
- ⁹ *G.I. Budker Institute of Nuclear Physics SB RAS (BINP), Novosibirsk 630090, Russia*
- ¹⁰ *GSI Helmholtzcentre for Heavy Ion Research GmbH, D-64291 Darmstadt, Germany*
- ¹¹ *Guangxi Normal University, Guilin 541004, People's Republic of China*
- ¹² *GuangXi University, Nanning 530004, People's Republic of China*
- ¹³ *Hangzhou Normal University, Hangzhou 310036, People's Republic of China*
- ¹⁴ *Helmholtz Institute Mainz, Johann-Joachim-Becher-Weg 45, D-55099 Mainz, Germany*
- ¹⁵ *Henan Normal University, Xinxiang 453007, People's Republic of China*
- ¹⁶ *Henan University of Science and Technology, Luoyang 471003, People's Republic of China*
- ¹⁷ *Huangshan College, Huangshan 245000, People's Republic of China*
- ¹⁸ *Hunan University, Changsha 410082, People's Republic of China*
- ¹⁹ *Indiana University, Bloomington, Indiana 47405, USA*
- ²⁰ *(A)INFN Laboratori Nazionali di Frascati, I-00044, Frascati, Italy; (B)INFN and University of Perugia, I-06100, Perugia, Italy*
- ²¹ *(A)INFN Sezione di Ferrara, I-44122, Ferrara, Italy; (B)University of Ferrara, I-44122, Ferrara, Italy*
- ²² *Johannes Gutenberg University of Mainz, Johann-Joachim-Becher-Weg 45, D-55099 Mainz, Germany*
- ²³ *Joint Institute for Nuclear Research, 141980 Dubna, Moscow region, Russia*
- ²⁴ *Justus Liebig University Giessen, II. Physikalisches Institut, Heinrich-Buff-Ring 16, D-35392 Giessen, Germany*
- ²⁵ *KVI-CART, University of Groningen, NL-9747 AA Groningen, The Netherlands*
- ²⁶ *Lanzhou University, Lanzhou 730000, People's Republic of China*
- ²⁷ *Liaoning University, Shenyang 110036, People's Republic of China*
- ²⁸ *Nanjing Normal University, Nanjing 210023, People's Republic of China*
- ²⁹ *Nanjing University, Nanjing 210093, People's Republic of China*
- ³⁰ *Nankai University, Tianjin 300071, People's Republic of China*
- ³¹ *Peking University, Beijing 100871, People's Republic of China*
- ³² *Seoul National University, Seoul, 151-747 Korea*
- ³³ *Shandong University, Jinan 250100, People's Republic of China*
- ³⁴ *Shanghai Jiao Tong University, Shanghai 200240, People's Republic of China*
- ³⁵ *Shanxi University, Taiyuan 030006, People's Republic of China*
- ³⁶ *Sichuan University, Chengdu 610064, People's Republic of China*
- ³⁷ *Soochow University, Suzhou 215006, People's Republic of China*
- ³⁸ *Sun Yat-Sen University, Guangzhou 510275, People's Republic of China*
- ³⁹ *Tsinghua University, Beijing 100084, People's Republic of China*
- ⁴⁰ *(A)Istanbul Aydin University, 34295 Sefakoy, Istanbul, Turkey; (B)Dogus University, 34722 Istanbul, Turkey; (C)Uludag University, 16059 Bursa, Turkey*
- ⁴¹ *University of Chinese Academy of Sciences, Beijing 100049, People's Republic of China*
- ⁴² *University of Hawaii, Honolulu, Hawaii 96822, USA*
- ⁴³ *University of Minnesota, Minneapolis, Minnesota 55455, USA*
- ⁴⁴ *University of Rochester, Rochester, New York 14627, USA*
- ⁴⁵ *University of Science and Technology Liaoning, Anshan 114051, People's Republic of China*
- ⁴⁶ *University of Science and Technology of China, Hefei 230026, People's Republic of China*
- ⁴⁷ *University of South China, Hengyang 421001, People's Republic of China*
- ⁴⁸ *University of the Punjab, Lahore-54590, Pakistan*
- ⁴⁹ *(A)University of Turin, I-10125, Turin, Italy; (B)University of Eastern Piedmont, I-15121, Alessandria, Italy; (C)INFN, I-10125, Turin, Italy*
- ⁵⁰ *Uppsala University, Box 516, SE-75120 Uppsala, Sweden*

⁵¹ Wuhan University, Wuhan 430072, People's Republic of China

⁵² Zhejiang University, Hangzhou 310027, People's Republic of China

⁵³ Zhengzhou University, Zhengzhou 450001, People's Republic of China

^a Also at State Key Laboratory of Particle Detection and Electronics, Beijing 100049, Hefei 230026, People's Republic of China

^b Also at Ankara University, 06100 Tandogan, Ankara, Turkey

^c Also at Bogazici University, 34342 Istanbul, Turkey

^d Also at the Moscow Institute of Physics and Technology, Moscow 141700, Russia

^e Also at the Functional Electronics Laboratory, Tomsk State University, Tomsk, 634050, Russia

^f Also at the Novosibirsk State University, Novosibirsk, 630090, Russia

^g Also at the NRC "Kurchatov Institute", PNPI, 188300, Gatchina, Russia

^h Also at University of Texas at Dallas, Richardson, Texas 75083, USA

ⁱ Also at Istanbul Arel University, 34295 Istanbul, Turkey

(Dated: February 25, 2016)

We present the first search for the rare decay of η' into $K^\pm\pi^\mp$ in $J/\psi \rightarrow \phi\eta'$, using a sample of 1.3×10^9 J/ψ events collected with the BESIII detector. No significant signal is observed, and the upper limit at the 90% confidence level for the ratio $\frac{\mathcal{B}(\eta' \rightarrow K^\pm\pi^\mp)}{\mathcal{B}(\eta' \rightarrow \gamma\pi^+\pi^-)}$ is determined to be 1.3×10^{-4} . In addition, we report the measurement of the branching fraction of $J/\psi \rightarrow \phi\eta'$ to be $(5.10 \pm 0.03(\text{stat.}) \pm 0.32(\text{syst.})) \times 10^{-4}$, which agrees with previous results from BESII.

PACS numbers: 13.25.Gv, 13.66.Bc, 14.40.Df, 12.38.Mh

I. INTRODUCTION

Non-leptonic weak decays are valuable tools for testing the Standard Model (SM), the Kobayashi-Maskawa (KM) mechanism, and the unitarity of the Cabibbo-Kobayashi-Maskawa (CKM) matrix, and for exploring physics beyond the SM. Among non-leptonic decays, the decay of the light pseudoscalar meson $\eta' \rightarrow K^\pm\pi^\mp$ is interesting because it is fundamental to understand the long-standing problem of the $\Delta I = 1/2$ rule in weak non-leptonic interactions.

The experimental $\Delta I = 1/2$ rule was first established in the decay $K \rightarrow \pi\pi$. A neutral kaon may decay into two pions with amplitudes A_0 or A_2 , respectively. As the real parts of these amplitudes, $\text{Re}A_0$ is dominated by $\Delta I = 1/2$ transitions and $\text{Re}A_2$ receives contributions from $\Delta I = 3/2$ transitions, the former transitions dominate $\text{Re}A_0$, which expresses the so-called $\Delta I = 1/2$ rule [1, 2]

$$\frac{\text{Re}A_0}{\text{Re}A_2} = 22.35. \quad (1)$$

Despite nearly 50 years of efforts, the microscopic dynamical mechanism responsible for such a striking phenomenon is still elusive. The decay $\eta' \rightarrow K^\pm\pi^\mp$ receives contributions from both the $\Delta I = 1/2$ and $\Delta I = 3/2$ parts of the weak hamiltonian [3]. It is possible to see whether the $\Delta I = 1/2$ rule is functional in this type of decay, and this could shed light on the origin of this rule. The branching fraction of $\eta' \rightarrow K^\pm\pi^\mp$ decay is predicted to be of the order of 10^{-10} or higher [3], with a large long-range hadronic contribution expected, which should become observable in high luminosity electron-positron collisions.

At present, there is no experimental information on the decay $\eta' \rightarrow K^\pm\pi^\mp$. The world's largest sample of 1.3×10^9 J/ψ events produced at rest and collected with the BESIII detector therefore offers a good opportunity to search for this rare decay. In this paper, the measurement of the ratio $\frac{\mathcal{B}(\eta' \rightarrow K^\pm\pi^\mp)}{\mathcal{B}(\eta' \rightarrow \gamma\pi^+\pi^-)}$ is presented, where the η' is produced in the decay $J/\psi \rightarrow \phi\eta'$. The advantage of comparing these two η' decay channels is that parts of the systematic uncertainties due to the tracking, the particle identification (PID), the branching fractions $\mathcal{B}(J/\psi \rightarrow \phi\eta')$ and $\mathcal{B}(\phi \rightarrow K^+K^-)$, and the number of J/ψ events cancel in the ratio. A measurement of the branching fraction $J/\psi \rightarrow \phi\eta'$ is also presented in which ϕ is reconstructed in its K^+K^- decay mode and η' is detected in the $\gamma\pi^+\pi^-$ decay mode. This can be compared with the results reported by the BESII [4], MarkIII [5], and DM2 [6] collaborations.

II. DETECTOR AND MONTE CARLO SIMULATION

BEPCII is a double-ring e^+e^- collider designed to provide a peak luminosity of $10^{33} \text{ cm}^{-2}\text{s}^{-1}$ at the center-of-mass (c.m.) energy of 3.770 GeV. The BESIII [7] detector, with a geometrical acceptance of 93% of the 4π stereo angle, is operating in a magnetic field of 1.0 T provided by a superconducting solenoid magnet. It is composed of a helium-based drift chamber (MDC), a plastic scintillator Time-Of-Flight (TOF) system, a CsI(Tl) electromagnetic Calorimeter (EMC) and a multi-layer resistive plate chamber (RPC) muon counter system (MUC).

Monte Carlo (MC) simulations are used to determine

the mass resolutions and detection efficiencies. The GEANT4-based simulation software BOOST [8] includes the geometric and material description of the BESIII detector, the detector response, and the digitization models, as well as the detector running conditions and performance. The production of the J/ψ resonance is simulated with the MC event generator KKMC [9, 10], while the decays are generated by EVTGEN [11] for known decay modes with branching fractions set to the Particle Data Group (PDG) [12] world average values, and by LUNDCHARM [13] for the remaining unknown decays. The analysis is performed in the framework of the BESIII offline software system (BOSS) [14].

III. DATA ANALYSIS

A. $J/\psi \rightarrow \phi\eta'$, $\eta' \rightarrow \gamma\pi^+\pi^-$

For the decay $J/\psi \rightarrow \phi\eta'$, $\phi \rightarrow K^+K^-$, $\eta' \rightarrow \gamma\pi^+\pi^-$, candidate events are selected by requiring four well reconstructed charged tracks and at least one isolated photon in the EMC. The four charged tracks are required to have zero net charge. Each charged track, reconstructed using hits in the MDC, is required to be in the polar angle range $|\cos\theta| < 0.93$ and pass within ± 10 cm of the interaction point along the beam direction, and within ± 1 cm in the plane perpendicular to the beam, with respect to the interaction point. For each charged track, information from the TOF and the specific ionization measured in the MDC (dE/dx) are combined to form PID confidence levels (C.L.) for the K , π and p hypotheses, and the particle type with the highest C.L. is assigned to each track. Two of the tracks are required to be identified as kaons and the remaining two tracks as pions.

Photon candidates are reconstructed by clusters of energy deposited in the EMC. The energy deposited in the TOF counter in front of the EMC is included to improve the reconstruction efficiency and the energy resolution. Photon candidates are required to have a deposited energy larger than 25 MeV in the barrel region ($|\cos\theta| < 0.80$) and 50 MeV in the end-cap region ($0.86 < |\cos\theta| < 0.92$). EMC cluster timing requirements are used to suppress electronic noise and energy deposits that are unrelated to the event. To eliminate showers associated with charged particles, the angle between the cluster and the nearest track must be larger than 15° .

A four-constraint (4C) kinematic fit is performed to the $\gamma K^+K^-\pi^+\pi^-$ hypothesis. For events with more than one photon candidate, the candidate combination with the smallest χ_{4C}^2 is selected, and it is required that $\chi_{4C}^2 < 50$.

The scatter plot of $M(\gamma\pi^+\pi^-)$ versus $M(K^+K^-)$ is shown in Fig. 1, where the $J/\psi \rightarrow \phi\eta'$ decay is clearly visible. To extract the number of $\phi\eta'$ events, an unbinned extended maximum likelihood fit is performed to the $M(\gamma\pi^+\pi^-)$ versus $M(K^+K^-)$ dis-

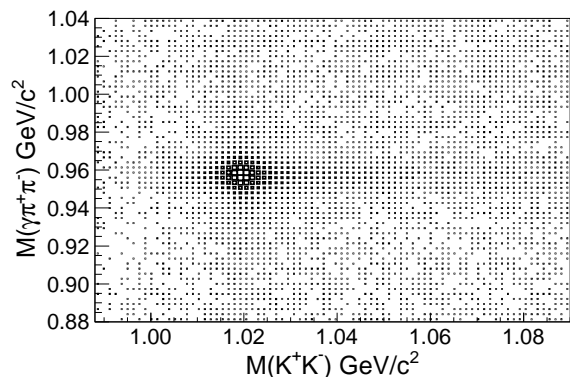


FIG. 1. Scatter plot of $M(\gamma\pi^+\pi^-)$ versus $M(K^+K^-)$.

tribution with the requirements of $0.988 \text{ GeV}/c^2 < M(K^+K^-) < 1.090 \text{ GeV}/c^2$ and $0.880 \text{ GeV}/c^2 < M(\gamma\pi^+\pi^-) < 1.040 \text{ GeV}/c^2$. Assuming zero correlation between the two discriminating variables $M(K^+K^-)$ and $M(\gamma\pi^+\pi^-)$, the composite probability density function (PDF) in the 2-dimensional fit is constructed as follows

$$\begin{aligned}
 F = & N_{\text{sig}} \times (F_{\text{sig}}^\phi \cdot F_{\text{sig}}^{\eta'}) \\
 & + N_{\text{bkg}}^{\text{non-}\eta'} \times (F_{\text{sig}}^\phi \cdot F_{\text{bkg}}^{\text{non-}\eta'}) \\
 & + N_{\text{bkg}}^{\text{non-}\phi} \times (F_{\text{bkg}}^{\text{non-}\phi} \cdot F_{\text{sig}}^{\eta'}) \\
 & + N_{\text{bkg}}^{\text{non-}\phi\eta'} \times (F_{\text{bkg}}^{\text{non-}\phi} \cdot F_{\text{bkg}}^{\text{non-}\eta'}).
 \end{aligned} \tag{2}$$

Here, the signal shape for ϕ (*i.e.* F_{sig}^ϕ) is modeled with a relativistic Breit-Wigner function convoluted with a Gaussian function taking into account the detector resolution; the signal shape for η' (*i.e.* $F_{\text{sig}}^{\eta'}$) is described by a normal Breit-Wigner function convoluted with a Gaussian function. The widths and masses of ϕ and η' are free parameters in the fit. The background shape of ϕ ($F_{\text{bkg}}^{\text{non-}\phi}$) is described by a second order Chebychev polynomial function, and the background shape of η' ($F_{\text{bkg}}^{\text{non-}\eta'}$) is described by a first order Chebychev polynomial function. All parameters related to the background shapes are free in the fit. N_{sig} is the number of $J/\psi \rightarrow \phi\eta'$, $\phi \rightarrow K^+K^-$, $\eta' \rightarrow \gamma\pi^+\pi^-$ signal events. The backgrounds are divided into three categories: non- $\phi\eta'$ background (*i.e.* $J/\psi \rightarrow \gamma K^+K^-\pi^+\pi^-$); non- ϕ -peaking background (*i.e.* $J/\psi \rightarrow K^+K^-\eta'$); and non- η' -peaking background (*i.e.* $J/\psi \rightarrow \phi\gamma\pi^+\pi^-$). The parameters $N_{\text{bkg}}^{\text{non-}\phi\eta'}$, $N_{\text{bkg}}^{\text{non-}\phi}$ and $N_{\text{bkg}}^{\text{non-}\eta'}$ are the corresponding three background yields.

The resulting fitted number of signal events is $N_{\text{sig}} = (31321 \pm 201)$; the projections of the fit on the $M(K^+K^-)$ and $M(\gamma\pi^+\pi^-)$ distributions are shown in Figs. 2 (a) and (b), respectively. The detection efficiency, $32.96 \pm 0.04\%$, is obtained from the MC simulation in which the angular distribution and the shape of $M(\pi^+\pi^-)$ are taken into account according to a previous BESIII measurement for $\eta' \rightarrow \pi^+\pi^-e^+e^-$ [15], where the non-resonant contribu-

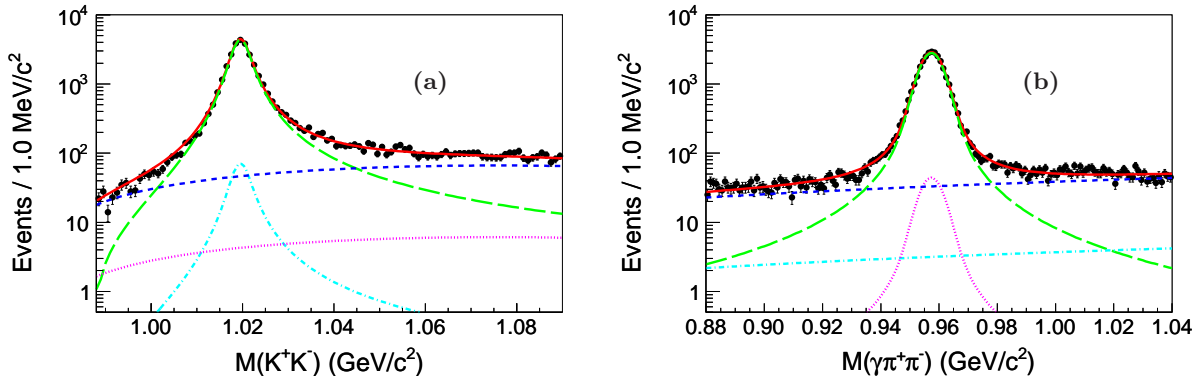


FIG. 2. Distributions of (a) $M(K^+K^-)$ and (b) $M(\gamma\pi^+\pi^-)$ with projections of the fit result superimposed for $J/\psi \rightarrow \phi\eta'$, $\phi \rightarrow K^+K^-$, $\eta' \rightarrow \gamma\pi^+\pi^-$. The dots with errors are for data, the solid curve shows the result of the fit to signal plus background distributions, the long-dashed curve is for $\phi\eta'$ signal, the dot-dashed curve shows the non- η' -peaking background, the dotted curve shows the non- ϕ -peaking background, and the short-dashed curve is for non- $\phi\eta'$ background.

tion (known as the “box anomaly”) is included in the simulation of $\eta' \rightarrow \gamma\pi^+\pi^-$.

B. $J/\psi \rightarrow \phi\eta'$, $\eta' \rightarrow K^\pm\pi^\mp$

To search for $\eta' \rightarrow K^\pm\pi^\mp$, the two-body decay $J/\psi \rightarrow \phi\eta'$ is chosen because of its simple event topology, $K^+K^-K^\pm\pi^\mp$, and because the narrow ϕ meson is easy to detect through $\phi \rightarrow K^+K^-$ decay. The selection criteria for the charged tracks are the same as that for the $J/\psi \rightarrow \phi\eta'$, $\eta' \rightarrow \gamma\pi^+\pi^-$ decay. Three tracks are required to be identified as kaons with the combination of TOF and dE/dx information and the remaining one is required to be identified as a pion.

A 4C kinematic fit imposing energy-momentum conservation is performed under the $K^+K^-K^\pm\pi^\mp$ hypothesis, and a requirement of $\chi_{4C}^2 < 50$ is imposed. To suppress the dominant background contamination from $J/\psi \rightarrow \phi\pi^+\pi^-$, the χ_{4C}^2 of the $K^+K^-K^\pm\pi^\mp$ hypothesis is required to be less than that for the $K^+K^-\pi^+\pi^-$ hypothesis. Candidates for $\phi \rightarrow K^+K^-$ are reconstructed from the K^+K^- combination with invariant mass closest to the nominal mass value. The remaining kaon together with the pion form the η' candidate.

Fig. 3 (a) shows the scatter plot to the invariant mass $M(K^+K^-)$ versus $M(K^\pm\pi^\mp)$. The process $\phi\eta'$ ($\eta' \rightarrow K^\pm\pi^\mp$) would result in an enhancement of events around the nominal masses of the ϕ and η' mesons, while no evident cluster is seen. Within three standard deviations of the ϕ mass, $|M(K^+K^-) - M(\phi)| < 15 \text{ MeV}/c^2$, the $K^\pm\pi^\mp$ invariant mass distribution is displayed in Fig. 3 (b); a few events are retained around the η' mass region, shown as the dots with error bars. To estimate the number of signal events passing the selection criteria, a region of $\pm 3\sigma$ around the η' nominal mass is selected, that is $|M(K^\pm\pi^\mp) - M(\eta')| < 7 \text{ MeV}/c^2$, where $\sigma = 2.2 \text{ MeV}$ is the mass resolution determined from MC simulation. Only one event survives in the signal region for further

analysis.

To investigate the potential background contributions, a study with an inclusive MC sample of 1.2×10^9 generic J/ψ decays is performed. It is found that the remaining background events mainly come from $J/\psi \rightarrow \phi\pi^+\pi^-$. Therefore an exclusive MC sample of 1.3×10^6 $J/\psi \rightarrow \phi\pi^+\pi^-$ events is generated in accordance with the partial wave analysis results of Ref. [16]. This sample corresponds to twice the expected $J/\psi \rightarrow \phi\pi^+\pi^-$ events in data. After normalizing to the world average value for $\mathcal{B}(J/\psi \rightarrow \phi\pi^+\pi^-)$, 2.0 events are expected in the $K\pi$ mass range of $[0.88, 1.04] \text{ GeV}/c^2$, with a total of 0.5 events in η' signal region, as shown by the solid histogram in Fig. 3 (b).

To conservatively estimate the upper limit, it is assumed that the only event in the signal region is a signal event. According to the Feldman-Cousins method [17], the corresponding upper limit of the number of events is $N^{\text{UL}} = 4.36$ at the 90% C.L.

IV. SYSTEMATIC UNCERTAINTIES

The systematic uncertainties in branching fraction measurement originate mainly from the differences of data and MC on tracking efficiency, photon reconstruction, PID efficiency, and the 4C kinematic fit, different fitting range and background shape, uncertainties from $\mathcal{B}(\phi \rightarrow K^+K^-)$ and $\mathcal{B}(\eta' \rightarrow \gamma\pi^+\pi^-)$, total number of J/ψ events and MC statistics. Other uncertainties related to the common selection criteria of the channels $J/\psi \rightarrow \phi\eta'$, $\eta' \rightarrow K^\pm\pi^\mp$ and $J/\psi \rightarrow \phi\eta'$, $\eta' \rightarrow \gamma\pi^+\pi^-$ cancel to first order in the ratio between the branching fractions.

The systematic uncertainties associated with the tracking efficiency and PID efficiency have been studied in the analysis of $J/\psi \rightarrow p\bar{p}\pi^+\pi^-$ and $J/\psi \rightarrow K_S^0 K^\pm\pi^\mp$ [18, 19]. The results indicate that the kaon/pion tracking and PID efficiencies for data agree with those of MC simula-

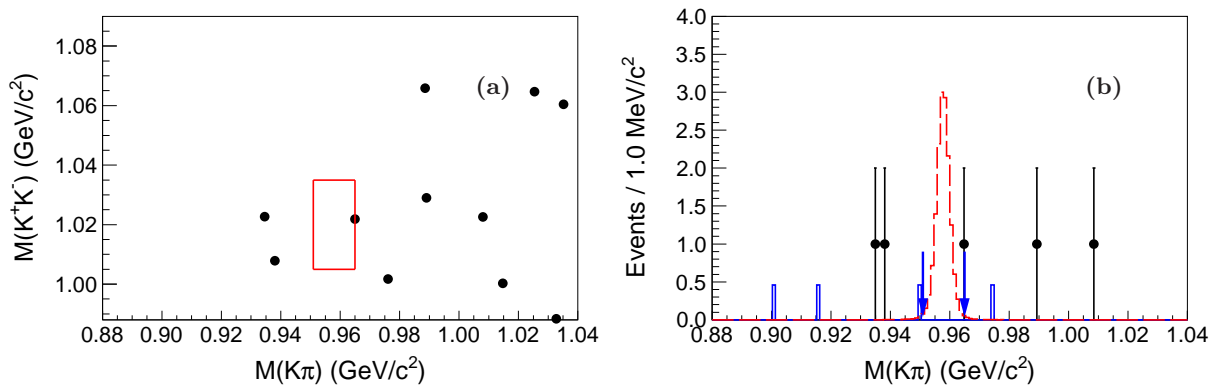


FIG. 3. (a) Scatter plot of $M(K^+K^-)$ versus $M(K^\pm\pi^\mp)$, where the box indicates the signal region with $|M(K^+K^-) - M(\phi)| < 15 \text{ MeV}/c^2$ and $|M(K^\pm\pi^\mp) - M(\eta')| < 7 \text{ MeV}/c^2$. (b) The $K^\pm\pi^\mp$ invariant mass distribution, where the arrows show the signal region. The dots with error bars are for data, the dashed histogram is for the signal MC with arbitrary normalization, and the solid histogram is the background contamination from a MC simulation of $J/\psi \rightarrow \phi\pi^+\pi^-$.

tion within 1%.

The photon detection is estimated by the study of $J/\psi \rightarrow \rho\pi$ [18]. The difference in the detection efficiency between data and MC is less than 1% per photon, which is taken as the systematic uncertainty because of the only photon in the $J/\psi \rightarrow \phi\eta', \eta' \rightarrow \gamma\pi^+\pi^-$ channel.

The uncertainty associated with the 4C kinematic fit comes from the difference between data and MC simulation. The method used in this analysis is to correct the tracking parameters of the helix fit to reduce the difference between MC and data, as described in Ref. [20]. This procedure yields a systematic uncertainty of 0.3% and 1.0% for the measurement of $\mathcal{B}(J/\psi \rightarrow \phi\eta')$ and the search of $\eta' \rightarrow K^\pm\pi^\mp$, respectively.

To estimate the systematic contribution due to the fit ranges, several alternative fits in different ranges are performed. The maximum difference on the number of signal events from alternative fits in different mass ranges is 0.1%, and this value is taken as systematic uncertainty. To estimate the systematic contribution due to the background shape, a fit is performed replacing the 2nd-order Chebychev polynomial function with an Argus function [21]; the change of signal yields is found to be 0.04%, which is negligible.

The decay $J/\psi \rightarrow \phi\eta', \phi \rightarrow K^+K^-, \eta' \rightarrow \gamma\pi^+\pi^-$ is used as control sample to estimate the uncertainty from the ϕ mass window criterion in the search of $\eta' \rightarrow K^\pm\pi^\mp$. The ϕ mass window criterion is applied to the control sample, and a fit is performed to $M(\gamma\pi^+\pi^-)$. After considering the efficiency difference, the difference of 1.2% in the number of signal events between this fit and the nominal 2D fit is taken as the uncertainty from the ϕ mass window.

The uncertainties on the intermediate-decay branching fractions of $\phi \rightarrow K^+K^-$ and $\eta' \rightarrow \gamma\pi^+\pi^-$ are taken from world average values [12].

The above systematic uncertainties together with the uncertainties due to the number of J/ψ events [22, 23] and MC statistics are all summarized in Table I, where

the uncertainties associated with MDC tracking, PID, branching fraction of $\phi \rightarrow K^+K^-$ cancel in the ratio $\frac{\mathcal{B}(\eta' \rightarrow K^\pm\pi^\mp)}{\mathcal{B}(\eta' \rightarrow \gamma\pi^+\pi^-)}$. The total systematic uncertainty is taken to be the sum in quadrature of the individual contributions.

V. RESULTS

At the 90% C.L., the upper limit on the ratio of $\mathcal{B}(\eta' \rightarrow K^\pm\pi^\mp)$ to $\mathcal{B}(\eta' \rightarrow \gamma\pi^+\pi^-)$ is given by

$$\frac{\mathcal{B}(\eta' \rightarrow K^\pm\pi^\mp)}{\mathcal{B}(\eta' \rightarrow \gamma\pi^+\pi^-)} < \frac{N^{\text{UL}} \cdot \varepsilon_{\gamma\pi^+\pi^-}}{N_{\text{sig}} \cdot \varepsilon_{K^\pm\pi^\mp}} \frac{1}{(1 - \sigma_{\text{syst}})}, \quad (3)$$

where N^{UL} is the upper limit of the number of observed events at the 90% C.L. for $\eta' \rightarrow K^\pm\pi^\mp$; $\varepsilon_{K^\pm\pi^\mp}$ and $\varepsilon_{\gamma\pi^+\pi^-}$ are the detection efficiencies of $J/\psi \rightarrow \phi\eta'$ for the two decays which are obtained from the MC simulations; σ_{syst} is the total systematic uncertainty in the search of $\eta' \rightarrow K^\pm\pi^\mp$. The 90% C.L. upper limit on the ratio $\frac{\mathcal{B}(\eta' \rightarrow K^\pm\pi^\mp)}{\mathcal{B}(\eta' \rightarrow \gamma\pi^+\pi^-)}$ is determined to be 1.3×10^{-4} by using the values of different parameters listed in Table II.

The branching fraction of $J/\psi \rightarrow \phi\eta'$ decay is calculated with the equation

$$\begin{aligned} \mathcal{B}(J/\psi \rightarrow \phi\eta') \\ = \frac{N_{\text{sig}}/\varepsilon_{\gamma\pi^+\pi^-}}{N_{J/\psi}\mathcal{B}(\eta' \rightarrow \gamma\pi^+\pi^-)\mathcal{B}(\phi \rightarrow K^+K^-)}, \end{aligned} \quad (4)$$

where $N_{J/\psi} = 1310.6 \times 10^6$ is the number of J/ψ events as determined by J/ψ inclusive hadronic decays [22, 23]. The obtained value for the branching fraction of $J/\psi \rightarrow \phi\eta'$ is $(5.10 \pm 0.03(\text{stat.}) \pm 0.32(\text{syst.})) \times 10^{-4}$.

TABLE I. Summary of systematic uncertainty sources and their contributions (in %).

Source	$\mathcal{B}(J/\psi \rightarrow \phi\eta')$	$\mathcal{B}(\eta' \rightarrow K^\pm\pi^\mp)/\mathcal{B}(\eta' \rightarrow \gamma\pi^+\pi^-)$
Tracking efficiency	4.0	-
PID efficiency	4.0	-
Photon reconstruction	1.0	1.0
4C kinematic fit	0.3	1.0
Fit range	0.1	0.1
Background shape	-	-
ϕ mass window	-	1.2
$\mathcal{B}(\phi \rightarrow K^+K^-)$	1.0	-
$\mathcal{B}(\eta' \rightarrow \gamma\pi^+\pi^-)$	2.0	-
$N_{J/\psi}$	0.8	-
MC statistic of $\eta' \rightarrow \gamma\pi^+\pi^-$	0.1	0.1
MC statistic of $\eta' \rightarrow K^\pm\pi^\mp$	-	0.1
Total	6.2	1.9

TABLE II. Values used in the calculations of the branching ratios, including the fitted signal yields, N (or 90% C.L. upper limit) and the detection efficiency, ε .

Decay mode	ε (%)	N
$\eta' \rightarrow K^\pm\pi^\mp$	36.75 ± 0.04	< 4.36 (90% C.L.)
$\eta' \rightarrow \gamma\pi^+\pi^-$	32.96 ± 0.04	31321 ± 201

VI. SUMMARY

Based on the 1.3×10^9 J/ψ events accumulated with the BESIII detector, a search for the non-leptonic weak decay $\eta' \rightarrow K^\pm\pi^\mp$ is performed for the first time through the $J/\psi \rightarrow \phi\eta'$ decay. No evidence for $\eta' \rightarrow K^\pm\pi^\mp$ is seen, and the 90% C.L. upper limit on the ratio of $\frac{\mathcal{B}(\eta' \rightarrow K^\pm\pi^\mp)}{\mathcal{B}(\eta' \rightarrow \gamma\pi^+\pi^-)}$ is measured to be 1.3×10^{-4} . Using the world average value of $\mathcal{B}(\eta' \rightarrow \gamma\pi^+\pi^-)$ [12], the corresponding upper limit on $\mathcal{B}(\eta' \rightarrow K^\pm\pi^\mp)$ is calculated to be 3.8×10^{-5} .

For the determination of the ratio of $\frac{\mathcal{B}(\eta' \rightarrow K^\pm\pi^\mp)}{\mathcal{B}(\eta' \rightarrow \gamma\pi^+\pi^-)}$, the $J/\psi \rightarrow \phi\eta'$ decay with $\phi \rightarrow K^+K^-$, $\eta' \rightarrow \gamma\pi^+\pi^-$ is analyzed and the corresponding branching fraction is $\mathcal{B}(J/\psi \rightarrow \phi\eta') = (5.10 \pm 0.03(\text{stat.}) \pm 0.32(\text{syst.})) \times 10^{-4}$. It is the most precise measurement to date and in agreement with the world average value.

ACKNOWLEDGMENTS

The BESIII collaboration thanks the staff of BEPCII and the IHEP computing center for their strong sup-

port. This work is supported in part by National Key Basic Research Program of China under Contract No. 2015CB856700; National Natural Science Foundation of China (NSFC) under Contracts Nos. 11125525, 11235011, 11322544, 11335008, 11425524, 11105101, 11205117, 11575133, 11175189; the Chinese Academy of Sciences (CAS) Large-Scale Scientific Facility Program; the CAS Center for Excellence in Particle Physics (CCEPP); the Collaborative Innovation Center for Particles and Interactions (CICPI); Joint Large-Scale Scientific Facility Funds of the NSFC and CAS under Contracts Nos. 11179007, U1232201, U1332201, U1232109; CAS under Contracts Nos. KJCX2-YW-N29, KJCX2-YW-N45; 100 Talents Program of CAS; National 1000 Talents Program of China; INPAC and Shanghai Key Laboratory for Particle Physics and Cosmology; German Research Foundation DFG under Contract No. Collaborative Research Center CRC-1044; Istituto Nazionale di Fisica Nucleare, Italy; Ministry of Development of Turkey under Contract No. DPT2006K-120470; Russian Foundation for Basic Research under Contract No. 14-07-91152; The Swedish Research Council; U. S. Department of Energy under Contracts Nos. DE-FG02-04ER41291, DE-FG02-05ER41374, DE-FG02-94ER40823, DESC0010118; U.S. National Science Foundation; University of Groningen (RuG) and the Helmholtzzentrum fuer Schwerionenforschung GmbH (GSI), Darmstadt; WCU Program of National Research Foundation of Korea under Contract No. R32-2008-000-10155-0.

- [1] M. Gell-Mann and A. H. Rosenfeld, Annu. Rev. Nucl. Sci. **7**, 407 (1957).
[2] Andrzej J. Buras, Jean-Marc Gerard and William A. Bardeen, Eur.Phys.J. C **74**, 2871 (2014).

- [3] L. Bergström and H. R. Rubinstein, Phys. Lett. B **203**, 183 (1988).
[4] M. Ablikim *et al.* (BESII Collaboration), Phys. Rev. D **71**, 032003 (2005).

- [5] D. Coffman *et al.* (MARKIII Collaboration), Phys. Rev. D **38**, 2695 (1988).
- [6] J. Jousset *et al.* (DM2 Collaboration), Phys. Rev. D **41**, 1389 (1990).
- [7] M. Ablikim *et al.* (BESIII Collaboration), Nucl. Instrum. Meth. A **614**, 345 (2010).
- [8] Z. Y. Deng *et al.*, Chinese Phys. C **30**, 371 (2006).
- [9] S. Jadach, B. F. L. Ward and Z. Was, Comput. Phys. Commun. **130**, 260 (2009).
- [10] S. Jadach, B. F. L. Ward and Z. Was, Phys. Rev. D **63**, 113009 (2001).
- [11] R. G. Ping, Chinese Phys. C **32**, 599 (2008); D. J. Lange, Nucl. Instrum. Meth. A **462**, 152 (2001).
- [12] K. A. Olive *et al.* (Particle Data Group), Chin. Phys. C **38**, 090001 (2014).
- [13] J. C. Chen, G. S. Huang, X. R. Qi, D. H. Zhang, and Y. S. Zhu, Phys. Rev. D **62**, 034003 (2000).
- [14] W. D. Li *et al.*, Proceeding of CHEP06, Mumbai, India (2006).
- [15] M. Ablikim *et al.* (BESIII Collaboration), Phys. Rev. D **87**, 092011 (2013).
- [16] M. Ablikim *et al.* (BESII Collaboration), Phys. Lett. B **607**, 243 (2005).
- [17] G. J. Feldman and R. D. Cousins, Phys. Rev. D **57**, 3873 (1998).
- [18] M. Ablikim *et al.* (BESIII Collaboration), Phys. Rev. D **83**, 112005 (2011).
- [19] M. Ablikim *et al.* (BESIII Collaboration), Phys. Rev. D **85**, 092012 (2012).
- [20] M. Ablikim *et al.* (BESIII Collaboration), Phys. Rev. D **87**, 012002 (2013).
- [21] H. Albrecht *et al.*, Phys. Lett. B **340**, 217 (1994).
- [22] M. Ablikim *et al.* (BESIII Collaboration), Chin. Phys. C **36**, 915 (2012).
- [23] With the same approach as for J/ψ events taken in 2009 (see Ref. [22] for more details), the preliminary number of J/ψ events taken in 2009 and 2012 is determined to be 1310.6×10^6 with an uncertainty of 0.8%.